MASTER

CONF-781234--2

EFFECTS OF DISSOLVED GAS AND DOWNSTREAM GEOMETRY DURING BLOWDOWN OF A SUBCOOLED LIQUID

by

Y. S. Cha and R. E. Henry

Prepared for

Symposium on Fluids Engineering 1978 Winter Annual Meeting

San Francisco, California

December 11-15, 1978

ARGONNE NATIONAL LABORATORY, ARGONNE, ILLINOIS

Operated under Contract W-31-109-Eng-38 for the

U. S. DEPARTMENT OF ENERGY

EFFECTS OF DISSOLVED GAS AND DOWNSTREAM GEOMETRY DURING BLOWDOWN OF A SUBCOOLED LIQUID

Y.S. Cha
R.E. Henry

Argonne National Laboratory

ABSTRACT

The effects of dissolved gas and downstream geometry during a blowdown transient were investigated experimentally. It was observed that dissolved gas did not significantly affect the blowdown process if no additional surface was available in the test section to provide nucleation sites. However, if sufficient nucleation sites were available in the system, large amplitude, continuous pressure oscillations were observed when the system contained a large amount of dissolved gas. The delay in blowdown times caused by these oscillations were between 20 to 30%. The amplitude of oscillations increased with increasing initial pressure in the blowdown vessel and the oscillatory frequency was between one to five cycles per second. These oscillations were likely to be associated with the so-called density-wave oscillations sometimes encountered in a two-phase flow system.

A single-phase, incompressible, quasi-steady model was developed to predict the pressure history in the blowdown vessel and the discharge flowrate. This model is able to predict the blowdown process as accurately as one can assess the polytropic behavior of the initial gas volume in the vessel.

NOMENCLATURE

A	cross-sectional area at the throat of the nozzle, m^2
C	nozzle discharge coefficient
d	diameter of the pipe downstream of the nozzle, m
f	friction factor
ℓ	length of the pipe downstream of the nozzle, m
m	mass, kg
n	polytropic exponent
P	pressure, Pa
Re	Reynolds number, $\rho_\ell U_1 d/\mu$
t	time, s
U	velocity, m/s
ν	specific volume, m^3/kg
V	volume, m^3
x	axial distance downstream from the nozzle, m
α	void fraction
ρ	density, kg/m^3
μ	viscosity, Pa.s
τ_o	skin friction, Pa
η	critical pressure ratio, P_t/P_i

Subscripts

A	atmospheric condition
B	blowdown
e	exit
g	gas
i	initial condition or inlet (stagnation) condition
ℓ	liquid
t	nozzle throat
o	blowdown vessel
1	location immediately downstream of the nozzle throat (see Fig. 2)
2,3,4	axial locations downstream of the nozzle throat (see Fig. 2)

INTRODUCTION

Emergency Core Cooling System (ECCS) accumulators of a Pressurized Water Reactor (PWR) contain water at approximately 65 C at pressures up to 4.24 MPa under steady-state conditions. The pressure is maintained with nitrogen gas, thus water can be saturated with nitrogen at that particular temperature and pressure. During a hypothetical Loss-of-Coolant Accident (LOCA), these high pressure accumulators would deliver water to the reactor pressure vessel. During this decompression process, the solution becomes supersaturated and dissolved nitrogen can exit from solution at active nucleation sites in the form of bubbles. These bubbles, in sufficient quantity, could significantly affect the discharge rate that is being delivered to the reactor by changing the compressible characteristics of the fluid. Experimental results reported by Westwater (1) indicated that homogeneous nucleation of the gas could not be achieved during a fast decompression process in a subcooled liquid. Therefore, the sites available for nucleation are limited by the availability of solid walls to provide active sites. In this study, the effects of dissolved gas during a blowdown transient are investigated. Three important parameters were varied in this investigation: (1) the amount of dissolved gas (N_2) in water, (2) the rate of depressurization, and (3) the number of preferred nucleation sites available in the system. The results presented in this paper were typical of a large amount of data obtained during this investigation which can be found in Ref. (2).

EXPERIMENTAL APPARATUS

Figure 1 illustrates the essential features of the apparatus which includes the blowdown vessel, the discharge nozzle, the piping system, and the instrumentation. The stainless steel blowdown vessel was approximately 1.22 m long and had an ID of 0.1 m. A bubbling device was installed at the bottom of the blowdown vessel to accelerate the dissolving process before each test. A relief valve (set at 4.93 MPa) was installed on top of blowdown vessel, and a vent line was provided at the top to alleviate the gas flow required for bubbling N_2 through the water. Absolute pressure transducers were used to measure the blowdown vessel and

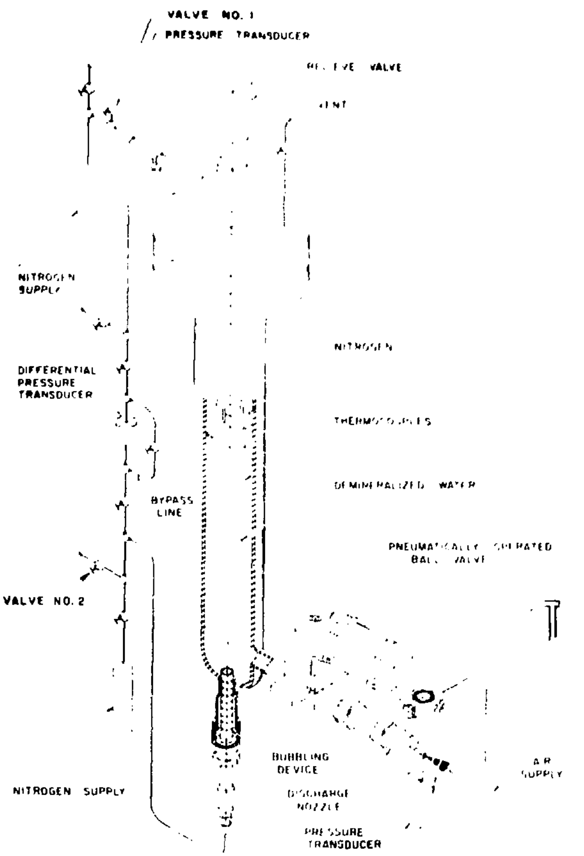

Fig.1 Schematic of experimental apparatus

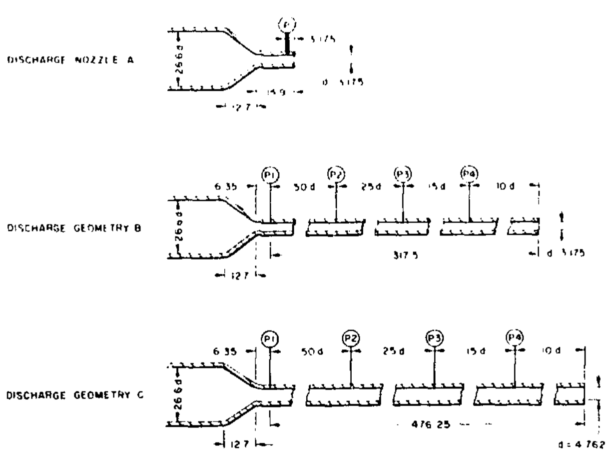

Fig.2 Dimensions (mm) and pressure tap locations for discharge geometries A, B, and C

discharge nozzle pressures, and three thermocouples were inserted into the blowdown vessel from the top to measure the gas space and water temperatures. The blowdown vessel was heated by externally wrapped heating wires and was thermally insulated in order to minimize heat loss during the nitrogen dissolving process. The transient was initiated by actuating a pneumatically operated ball valve upstream of the discharge nozzle. All measurements were recorded on a Honeywell visicorder (Model 1858).

Three discharge geometries which are shown in Fig. 2 were fabricated for these tests. Discharge nozzle A had a short parallel section downstream from the throat of the nozzle which had an ID of 3.175 mm, discharge geometry B had a long circular duct downstream from the throat of the nozzle with an ID of 3.175 mm, and discharge geometry C had a long circular duct downstream from the throat of the nozzle with an ID of 4.762 mm. Figure 2 also shows the locations of the pressure taps for each test section. The length-to-diameter ratio of the circular duct downstream of the throat was ~100 for both discharge geometries B and C.

Additional internal surface area (preferred nucleation sites) was provided in some tests by installing a tube bundle in the blowdown vessel. This tube bundle increased the surface area in contact with water by a factor of approximately 10, and was made of thin-walled hollow tubes. These tubes had an ID of 3.937 mm and an OD of 4.420 mm and were welded to three thin perforated plates. The tube bundle was fitted into the vessel from the top and stopped shortly before reaching the opening leading to the discharge nozzle.

EXPERIMENTAL PROCEDURES

Before pressurizing the system, the blowdown vessel was filled with dimineralized water to a level of approximately three-fourths of the total height of the blowdown vessel (only one water level was used for all the tests) and then heated up to the desired temperature (this procedure usually required less than one hour). The water temperature was then maintained constant by adjusting the rheostat settings (which controlled the power input to the heating wires) during the nitrogen dissolving (bubbling) process. Initially, three different pressurization procedures were employed: (1) zero contact time between N_2 and water, (2) 6 hours bubbling at the desired pressure, and (3) 48 hours bubbling at the desired pressure. In later tests, only two pressurization procedures were employed: (1) zero bubbling time, and (2) 24 hours bubbling since no difference could be discerned between the 24 and 48 hour intervals. During the bubbling process, the valve in the vent line was opened slightly.

Immediately before each test, the power supply to the heating wires, the vent line valve, and the nitrogen supply valve (valve No. 2 in Fig. 1) were turned off. The recorder was then turned on and the ball valve was actuated to initiate the blowdown.

The range of initial pressure in the blowdown vessel in the present tests were from 1.48 MPa to 4.24 MPa. All the tests were conducted by discharging the liquid into the atmosphere. Most tests were conducted at a temperature of 65 C and only a few tests were conducted at room temperature and at 38 C. This was done because results indicated temperature variations in this range had little effect on the blowdown behavior.

Since a large number of tests were conducted, it would be convenient to designate each test run with a name according to the particular conditions under which it was conducted. The designation adopted in this paper is:

> Run (R) - type of discharge nozzle (A, B, or C) - with or without tube bundle inside the blowdown vessel (TB or NO) - initial pressure in the blowdown vessel (MPa) - temperature (C) - bubbling time (hours).

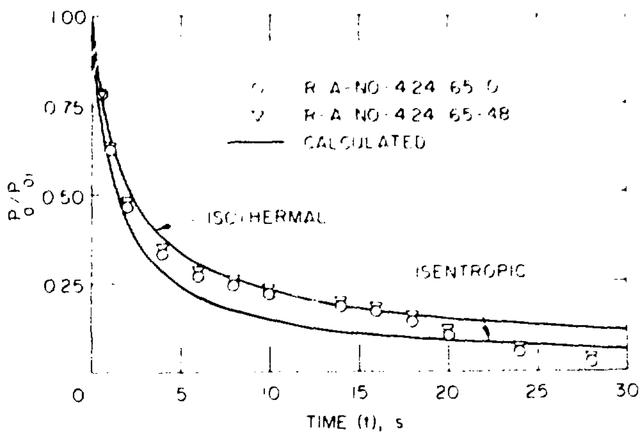

Fig.3 Comparison between calculated and measured vessel pressure versus time for tests conducted with discharge nozzle A and without tube bundle inside the vessel

For example, R-A-TB-4.24-65-24 represents a test run with discharge nozzle A, with a tube bundle inside the vessel, initial vessel pressure of 4.24 MPa, a water temperature of 65 C, and a system bubbling time of 24 hours at this temperature and pressure.

EXPERIMENTAL RESULTS

A. Test Results With Discharge Nozzle A

(1) Without Tube Bundle Inside the Blowdown Vessel. Figure 3 shows the typical variation of vessel pressure with time. In general, the vessel pressure decreased rapidly in the first few seconds and the rate of depressurization decreased with time. There were points of inflection in the vessel pressure versus time curves, which correspond roughly to the instant at the end of the blowdown test, i.e., the instant when the liquid above the height of the discharge nozzle in the blowdown vessel was exhausted. In this paper, the blowdown time was defined as the time required to exhaust all the liquid in the blowdown vessel above the discharge nozzle. Figure 3 shows that the decompression process of a nearly saturated solution (with 48 hours of gas bubbling) was slightly slower than that of an undersaturated solution (zero bubbling time).

Typical variations of the nozzle exit pressure with time are shown in Fig. 4. The nozzle exit pressure exhibited two peaks. The first peak occurred immediately (in the order of one-tenth of a second) after the ball valve was actuated and it decayed to atmospheric pressure in a relatively short period of time (in order of one second). The occurrence of this peak in nozzle exit pressure was probably due to the initial filling of the pressure tap line with water as it entered the test section. The second rise in nozzle exit pressure was simply due to the fact that the liquid in the blowdown vessel was exhausted and gas was being discharged. This occurred simultaneously with the inflection point in the vessel pressure versus time curve and provided an accurate means of determining the blowdown time for all the tests. In general, the higher the initial pressure, the shorter the blowdown time. Pressure pulses at relatively large intervals (similar to that shown in Fig. 8) were observed during early stage of the blowdown for tests with relatively high initial vessel pressure and with a large amount of nitrogen dissolved in water. These pulses were probably due to the formation of limited number of bubbles in

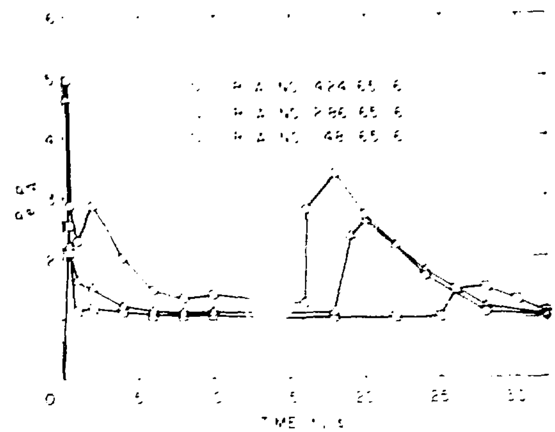

Fig.4 Experimentally determined nozzle exit pressure versus time for discharge nozzle A and without tube bundle inside the vessel

the system during the tests since there were cavities in the solid boundary of the system which can serve as nucleation sites. It can be shown analytically that if these cavities are large enough and contain sufficient amounts of trapped gas, bubbles of fairly large sizes can be formed in a relatively short period of time comparable to the blowdown time of the present tests (2). These bubbles would either rise to the surface or be carried downstream through the nozzle when the diameters of these bubbles become equivalent to the departure diameters.

Figure 5 shows the typical temperature variation in the gas region in the blowdown vessel. The measured gas temperature dropped slightly during the first few seconds, while the pressure was decreasing rapidly, and then recovered during the later stage of the test. From then on until the end of the test, the gas temperature remained constant. The temperature measured by the thermocouple in the gas region may not represent the true temperature of the expansion process since there may be some liquid droplets entrained in the gas space by the initial depressurization. These liquid droplets would be hotter than the gas and would heat the surface

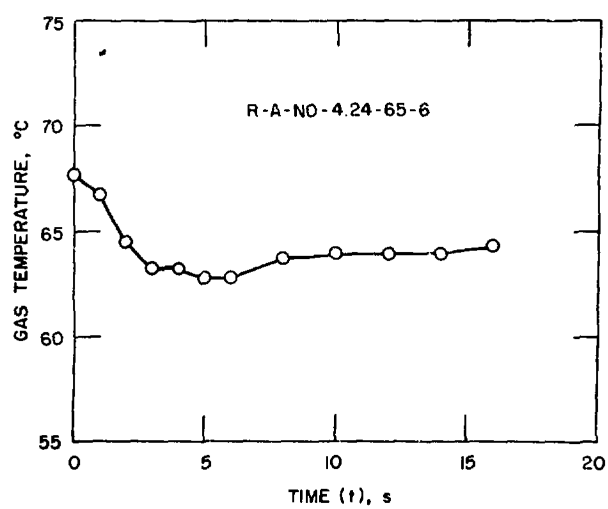

Fig.5 Measured variation of gas temperature with time for test conducted with discharge nozzle A and without tube bundle inside the vessel

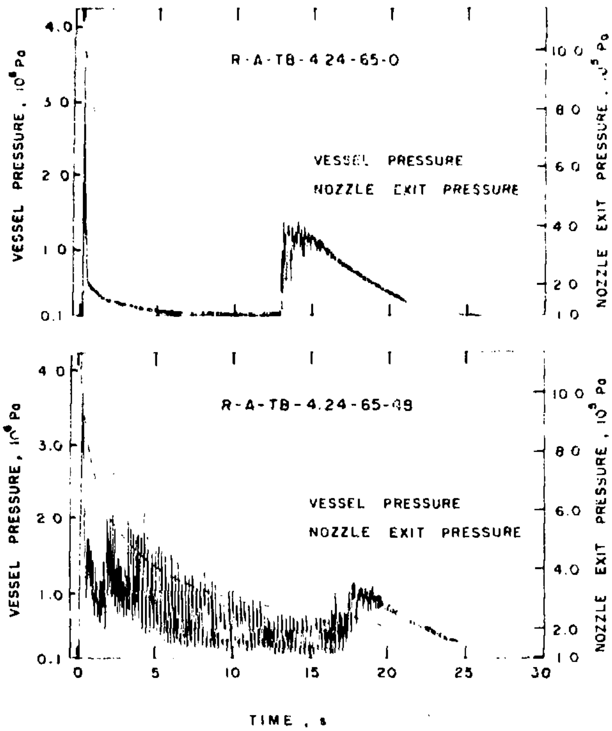

Fig.6 Measured vessel pressure and nozzle exit pressure versus time for tests conducted with discharge geometry A and with tube bundle inside the vessel

TABLE I. MEASURED BLOWDOWN TIMES FOR DISCHARGE NOZZLE A

Run Designation	$t_B'(s)$	$\Delta t(s)$	% Difference
R-A-NO-4.24-65-48	15.4	0.3	2.0
R-A-NO-4.24-65-0	15.1		
R-A-NO-2.86-65-48	19.0	1.2	6.7
R-A-NO-2.86-65-0	17.8		
R-A-NO-1.48-65-48	27.2	1.5	5.8
R-A-NO-1.48-65-0	25.7		
R-A-TB-4.24-65-48	16.3	3.1	23.5
R-A-TB-4.24-65-0	13.2		
R-A-TB-2.86-65-48	19.7	4.3	27.9
R-A-TB-2.86-65-0	15.4		
R-A-TB-1.48-65-48	28.0	5.5	24.4
R-A-TB-1.48-65-0	22.5		

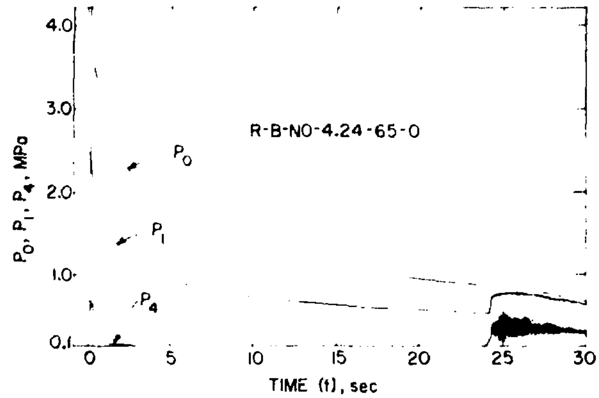

Fig.7 Variations of vessel pressure and pressures downstream of the nozzle throat with time for test conducted with discharge geometry B, without tube bundle inside the vessel, and with zero gas bubbling time

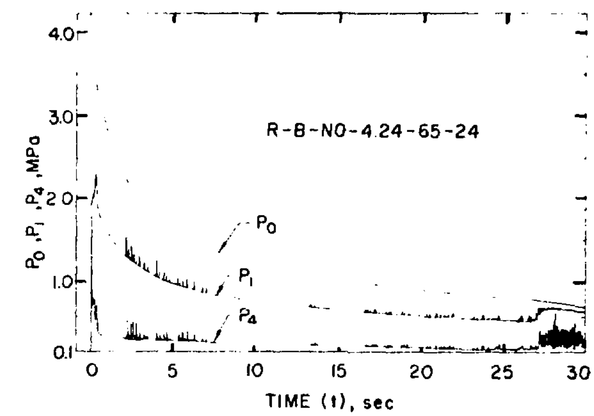

Fig.8 Variations of vessel pressure and pressures downstream of the nozzle throat for test conducted with discharge geometry B, without tube bundle inside the vessel and with 24 hour gas bubbling time

TABLE II. MEASURED BLOWDOWN TIMES FOR DISCHARGE GEOMETRY B

Run Designation	$t_B(s)$	$\Delta t_B(s)$	% Difference
R-B-NO-4.24-65-24	26.9	2.7	11.1
R-B-NO-4.24-65-0	24.2		
R-B-NO-2.86-65-24	32.9	3.9	13.4
R-B-NO-2.86-65-0	29.0		
R-B-NO-1.48-65-24	43.6	1.6	3.8
R-B-NO-1.48-65-0	42.0		
R-B-TB-4.24-65-24	27.0	5.1	23.3
R-B-TB-4.24-65-0	21.9		
R-B-TB-2.86-65-24	31.9	5.0	18.6
R-B-TB-2.86-65-0	26.9		
R-B-TB-1.48-65-24	44.5	4.2	10.4
R-B-TB-1.48-65-0	40.3		

of the thermocouple if initimate contact was e-tablished. The gas was also receiving heat from the vessel walls (by conduction) during the test. In general, it was observed that the higher the initial pressure, the larger the temperature drop during the initial phase of the blowdown process.

(ii) With Tube Bundle Inside the Blowdown Vessel. Figure 6 shows the comparison of the test results between a zero bubbling time and a 48 hour bubbling time. Results similar to that without the tube bundle inside the blowdown vessel were observed for tests with zero bubbling time. However, large amplitude oscillations (in the order of several atmospheres) of the nozzle exit pressure were observed for tests with 48 hours bubbling time. The amplitude of the oscillations decreased with decreasing initial pressure (hence, the pressure drop across the nozzle) in the blowdown vessel. The oscillatory frequency was approximately 4-5 Hz and appeared to decrease slightly during the later stages of the blowdown process. It was observed that the shape of the jet at the nozzle exit was alternating between a relatively stable circular-column and a dispersed circular-cone. The ratios between the peak of the oscillating nozzle exit pressure and the corresponding vessel pressure at any instant ranged from 0.25 to 0.30 for those tests with initial pressure equal to 2.86 MPa or higher. The ratio was slightly lower for tests with initial pressure equal to 1.48 MPa.

The delay in the blowdown process caused by these large amplitude pressure oscillations was more pronounced than those tests conducted without tube bundles inside the blowdown vessel. Table I is a list of the measured blowdown times of the tests conducted with discharge nozzle A. It can be observed from Table I that the effect of dissolved nitrogen was to increase the blowdown time by approximately 5 percent for tests without a tube bundle inside the vessel whereas it increased the blowdown time by approximately 25 percent for tests with the tube bundle inside the vessel. In cases with no gas bubbling, the blowdown times for tests with the tube bundle installed were shorter than those without the tube bundle. This reflects a smaller liquid volume because of the presence of tube bundle in the former cases.

B. Test Results With Discharge Geometries B and C

(i) Without Tube Bundle Inside the Blowdown Vessel. Figure 7 and Fig. 8 show the measured vessel pressure and pressures downstream from the nozzle throat for tests conducted with discharge geometry B (only P_1 and P_4 are shown since P_2 and P_3 exhibited similar behaviors). Smooth variations in pressures were observed for tests with zero bubbling time. This is typical for all the tests with no gas bubbling. For tests with 24 hours bubbling time, nonperiodic, intermittent oscillations (at relatively large intervals) with relatively small amplitudes were observed for the pressures in the constant cross-sectional area portion of the test section. Similar behaviors were observed for tests conducted with discharge geometry C. The blowdown times for these tests are listed in Tables II and III. The percentage increase in blowdown time, between tests with zero bubbling time and 24 hour bubbling time, was approximately 10% for relatively high initial pressures in the blowdown vessel and approximately 5% for low initial pressure in the blowdown vessel. The percentage increase in blowdown time for these tests were slightly higher than that of the corresponding tests conducted with discharge nozzle A. This is because the long pipe downstream of the nozzle provided additional flow resistance as illustrated by the larger discharge times with no dissolved gas. For example, a comparison between results shown in Table I and Table II (keep in mind that discharge geometries A and B had the same throat diameter) indicated that the blowdown time was increased appreciably by the addition of a long pipe downstream of the nozzle. However, the available nucleation sites in the system were not enough to produce the large amplitude, continuous, and nearly periodic oscillations observed for tests conducted with tube bundle inside the vessel.

TABLE III. MEASURED BLOWDOWN TIMES FOR DISCHARGE GEOMETRY C

Run Designation	t_B(s)	Δt_B(s)	% Difference
R-C-NO-4.24-65-24	13.9	1.6	13.0
R-C-NO-4.24-65-0	12.3		
R-C-NO-2.86-65-24	16.2	1.4	9.45
R-C-NO-2.86-65-0	14.8		
R-C-NO-1.48-65-24	21.9	0.9	4.28
R-C-NO-1.48-65-0	21.0		
R-C-TB-4.24-65-24	13.7	3.4	33.0
R-C-TB-4.24-65-0	10.3		
R-C-TB-2.86-65-24	16.2	3.0	22.7
R-C-TB-2.86-65-0	13.2		
R-C-TB-1.48-65-24	21.0	2.9	16.0
R-C-TB-1.48-65-0	18.1		

(ii) With Tube Bundle Inside the Blowdown Vessel. Figure 9 and Fig. 10 show the measured vessel pressure and pressures downstream from the nozzle throat for tests conducted with discharge geometry B. Again, smooth pressure profiles were observed for tests with no gas bubbling. Large amplitude oscillations occurred in the pipe downstream of the nozzle throat for tests with 24 hour bubbling time. The oscillatory frequency decreased slightly during the later stage of the blowdown process. The amplitude of oscillations were observed to decrease with decreasing initial pressure in the blowdown vessel. Again, the shape of the jet at the exit was observed to alternate between circular-column and circular-cone when oscillations occurred. Similar behavior was observed for tests conducted with discharge geometry C.

The blowdown times for these tests are listed in Tables II and III. The delays in blowdown time caused by flow oscillations were between 20 to 30 per cent for tests with relatively high initial pressure and were between 10 to 15 per cent for tests with low initial pressures in the blowdown vessel.

Figure 11 shows the comparison of the variation of the average pressure with distance in the constant area portion of the test section for a test with oscillations and one without oscillation at two instants. For the test without oscillations (zero bubbling time), the pressure was observed to decrease fairly linearly with the axial distance downstream from the nozzle throat. For tests with oscillations (24 hour bubbling time), the pressure was no longer a linear function of axial distance and the pressure gradient increased slightly along the axial distance. This was caused by the increase in velocity as a result of increase in void fraction along the axial distance.

A SINGLE-PHASE, INCOMPRESSIBLE, QUASI-STEADY MODEL

Assuming that the diameters of the vessel and the pipe upstream of the nozzle are much larger than that of the pipe downstream of the nozzle and the void fraction is extremely small so that single-phase incompressible flow results can be applied. The discharge velocity at any instant is given approximately by:

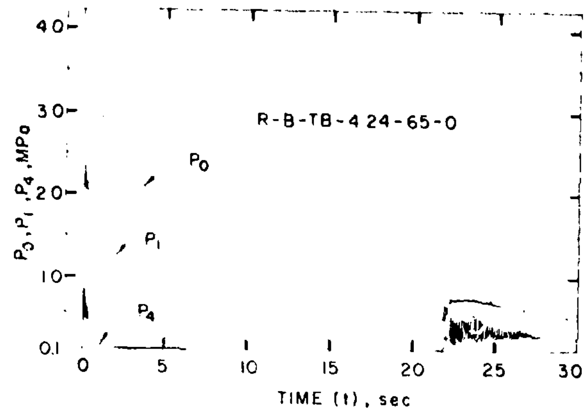

Fig.9 Variations of vessel pressure and pressures downstream of the nozzle throat for test conducted with discharge geometry B, with tube bundle inside the vessel, and with zero gas bubbling time

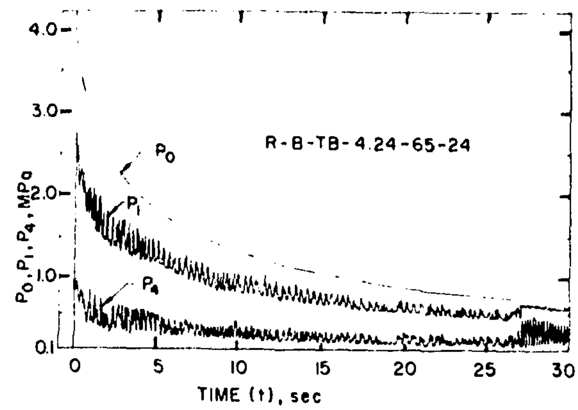

Fig.10 Variations of vessel pressure and pressures downstream of the nozzle throat for test conducted with discharge geometry B, with tube bundle inside the vessel, and with 24 hour gas bubbling time

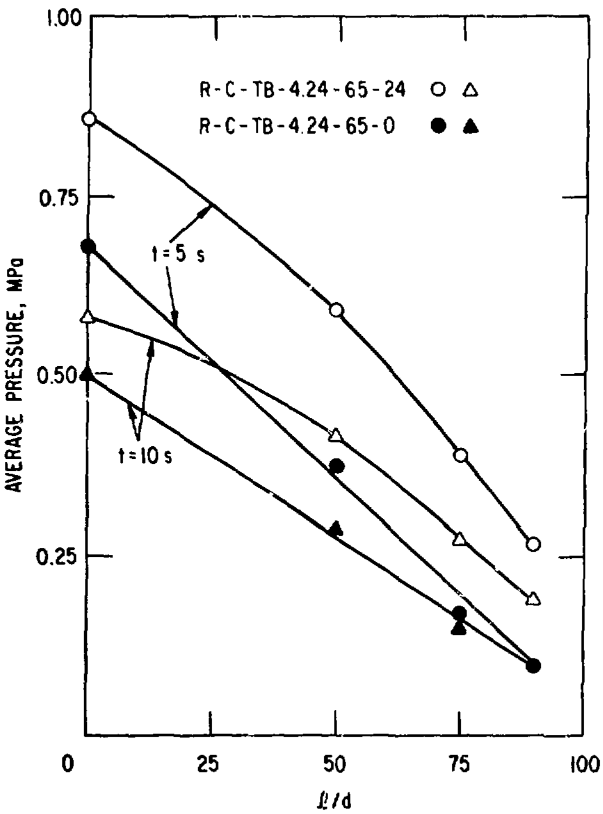

Fig.11 Comparison of the average pressure versus axial distance downstream from the nozzle throat between test with continuous pressure oscillations and test without continuous pressure oscillations at two instants

$$U_1 = C[2(P_o - P_1)v_\ell]^{1/2} \tag{1}$$

The rate of change of liquid mass in the vessel can be approximated by:

$$dm_\ell/dt = -AU_1\rho_\ell \tag{2}$$

for small void fractions. Since the total volume of the vessel remains unchanged, thus,

$$V = V_g + V_\ell = v_g m_g + v_\ell m_\ell$$

and

$$dV = v_g dm_g + m_g dv_g + v_\ell dm_\ell + m_\ell dv_\ell = 0 \tag{3}$$

Assuming that no mass transfer occurred at the liquid-gas interface and the liquid flow is incompressible:

$$dm_g = dv_\ell = 0 \tag{4}$$

Equation (3) becomes:

$$dV/dt = v_\ell(dm_\ell/dt) + m_g(dv_g/dt) = 0 \tag{5}$$

Substituting equation (2) into equation (5);

$$AU_1 = m_g(dv_g/dt) \tag{6}$$

Assuming that the gas in the vessel expands polytropically,

$$P_o v_g^n = \text{constant} = P_{oi} v_{gi}^n \tag{7}$$

Then,

$$dv_g/dt = -v_g(dP_o/dt)/nP_o \tag{8}$$

Substituting equations (7) and (8) into equation (6),

$$dP_o/dt = -AU_1 nP_o^{(1+1/n)}/(V_{gi}P_{oi}^{1/n}) \tag{9}$$

where

$$V_{gi} = m_\ell v_{gi} \tag{10}$$

The equation of motion for one-dimensional, incompressible, unsteady flow in a conduit is (3),

$$(\partial P/\partial x)/\rho_\ell + 4\tau_o/(\rho_\ell d) + dU_1/dt = 0 \quad (11)$$

where

$$\tau_o = \rho_\ell f U_1^2/8 \quad (12)$$

The steady-state friction factor is usually used for f (3). In the present analysis, we shall assume that the flow in the pipe is turbulent and employ the Blasius equation for f:

$$f = 0.3164/Re^{0.25} \quad (13)$$

From the experimental results, we see that the pressure gradient at any instant in the pipe is nearly constant for cases where the flow is incompressible. Therefore, it can be assumed that,

$$\partial P/\partial x = (P_e - P_1)\ell \quad (14)$$

Substituting equations (1), (13), and (14) into equation (11),

$$(P_e - P_1)/\ell + 0.3164\ C^2(P_o - P_1)/(Re^{0.25}d) +$$

$$C^2(dP_o/dt - dP_1/dt)/U_1 = 0 \quad (15)$$

Equations (1), (9), and (15) can be employed to solve for the three unknowns U_1, P_o, and P_1 with the following initial conditions,

$$P_o = P_{oi},\ P_1 = P_e = P_A;\quad \text{at } t = 0 \quad (16)$$

Under most circumstances, the third term is small compared to the first two terms on the left hand side of equation (15), thus equation (15) can be approximated by

$$(P_e - P_1)/\ell + 0.3164\ C^2(P_o - P_1)/(Re^{0.25}d) = 0 \quad (17)$$

Substituting equations (1) and (17) into equation (9),

$$\frac{dP_o}{dt} = -\left[\frac{nACP_o^{(1+1/n)}}{V_{gi}P_{oi}^{1/n}}\right] \times \left[\frac{2\nu_\ell(P_o - P_e)}{1 + 0.3164\ C^2\ell/(Re^{0.25}d)}\right]^{1/2} \quad (18)$$

For the blowdown tests reported in this paper, the liquids were discharged into the atmosphere, therefore, if incompressible flow is assumed

$$P_e = P_A << P_o \quad (19)$$

The Reynolds number in the pipe ranged from 10^5 to 6 x 10^5 in the present tests. The corresponding friction factor for turbulent flow in smooth pipes ranges from 0.178 to 0.126. If one adopts an average value for the friction factor,

$$f = 0.3164/Re^{0.25} \approx 0.015 \quad (20)$$

then, equation (18) can be integrated directly by employing (19) and (20). This results in an algebraic equation for P_o,

$$\frac{P_o}{P_{oi}} = \left\{1 + \frac{AC(2+n)\left[\frac{2\nu_\ell P_{oi}}{1 + 0.015\ C^2\ell/d}\right]^{1/2} t}{2\ V_{gi}}\right\}^{-\left(\frac{2n}{2+n}\right)} \quad (21)$$

Comparisons between experimental results and calculated results by using equation (21) are shown in Figs. 3, 12, and 13. Since the discharge coefficient was not measured, the value of C was set equal to one in these calculations. During early stages of the blowdown transient, while the vessel pressure was decreasing rapidly, the gas in the vessel expanded in a manner which was

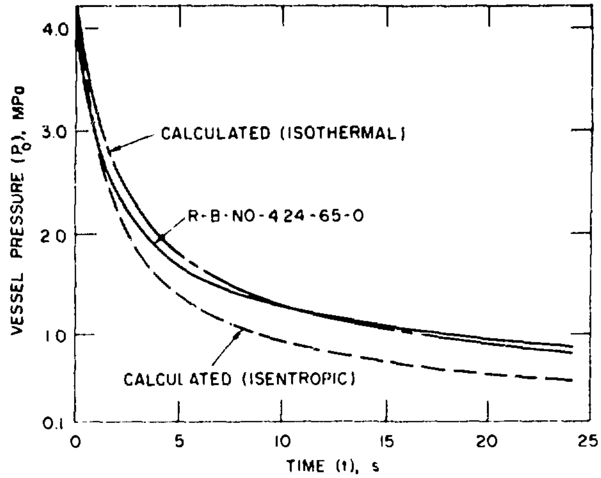

Fig.12 Comparison between calculated and measured vessel pressure versus time for test conducted with discharge geometry B, without tube bundle inside the vessel, and with zero gas bubbling time

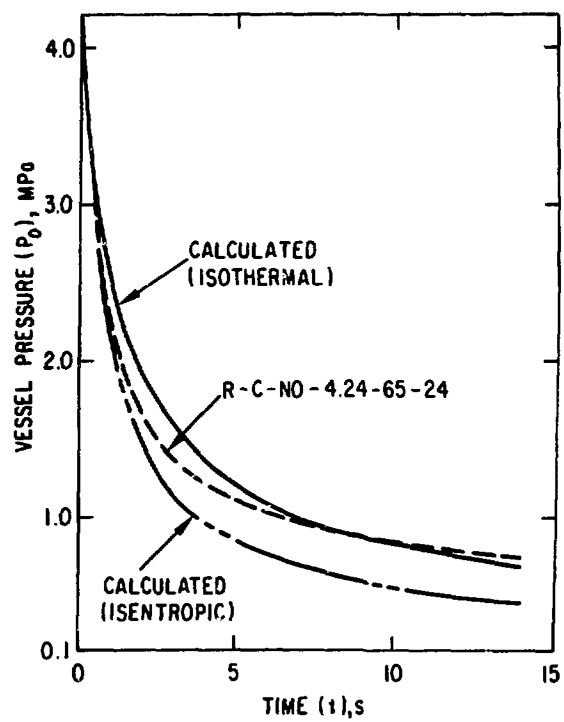

Fig.13 Comparison between calculated and measured vessel pressure versus time for test conducted with discharge geometry C, without tube bundle inside the vessel, and with 24 hour gas bubbling time

much closer to an isentropic (n = 1.40) process than an isothermal (n = 1.0) one. During later stages of the test, the gas in the vessel behaved in a manner much closer to an isothermal process. The blowdown time can be calculated by employing the following equation:

$$V_{\ell i} = \int_0^{t_B} AU_1 dt \qquad (22)$$

where $V_{\ell i}$ is the initial liquid volume above the level of the discharge nozzle in the blowdown vessel. Table IV shows the comparison between the calculated and the measured blowdown times for discharge geometry B. It can be observed that the measured blowdown times fell between that calculated by using n = 1.0 and n = 1.40. For high initial pressures in the blowdown vessel, which represent faster depressurization processes, the isentropic assumption provides a better prediction of the blowdown times. For relatively low initial pressures in the blowdown vessel, the isothermal assumption provides a better agreement.

Figure 14 shows the comparison of the calculated time history of the blowdown vessel pressure between the approximate solution obtained by using equation (21) and the more exact solution obtained by simultaneously solving equations (9) and (15). It is obvious that the difference between these two solutions is small and begins to appear only during later stages of the blowdown process.

TABLE IV. COMPARISON BETWEEN CALCULATED AND MEASURED BLOWDOWN TIMES FOR DISCHARGE GEOMETRY B WITH C = 1

Run Designation	Calculated t_B(s) n = 1.0	Calculated t_B(s) n = 1.40	Measured t_B(s)
R-B-NO-4.24-65-0	19.9	25.9	24.2
R-B-NO-2.86-65-0	24.8	33.4	29.0
R-B-NO-1.48-65-0	37.7	64.4	42.0

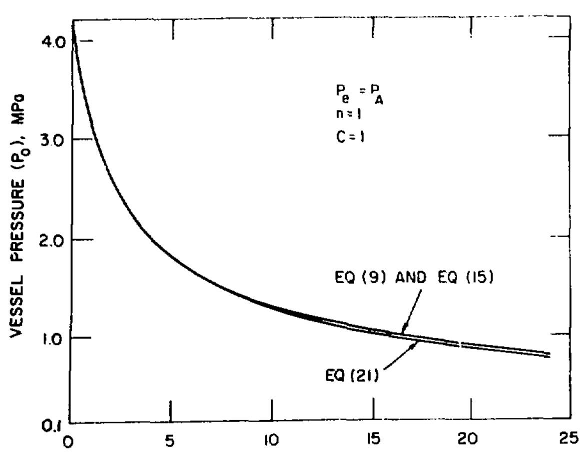

Fig.14 Comparison of the calculated variation of vessel pressure with time between employing the approximate solution provided by equation (21) and the more exact solution provided by equations (9) and (15)

DISCUSSIONS

The phenomenon of large amplitude, continuous pressure (and flow), oscillations observed experimentally is likely to be associated with two-phase instabilities. The frequency of oscillation of the present tests (1 to 5 Hz) seemed to suggest that the oscillations were the so-called density-wave oscillations. Density-wave oscillations in two-phase, two-component flow systems has been investigated both experimentally and analytically by Stenning and Veziroglu (4, 5). Their experimental set-up, which was very similar to the apparatus used in this study (discharge nozzle A), consisted mainly of a surge tank, an inlet duct, a mixer, an exit duct, and an orifice restriction. The mixer was, in fact, a bubbler inside a small plenum and air could be injected through the bubbler into the plenum and mixed there with the water flow from the surge tank. The two-phase mixture was then discharged into the atmosphere through the orifice. By increasing the air injection rate or by decreasing the water flow rate from the surge tank, the system could become unstable. The most important characteristic of density-wave oscillations is that the frequency of oscillations is inversely proportional to the residence time of the system. The residence time for the present system equals approximately the time required for the two-phase mixture to travel from the vessel to the nozzle inlet (the distance is approximately 298.5 mm). Simple calculations (2) indicated that the frequency was approximately one cycle per second for the present system which is of the same order of magnitude of the experimentally observed frequency.

The oscillations and the change in shape of the jet at the exit can be explained from two different viewpoints depending on the void fraction of the system which was, unfortunately, not measured. Stenning and Veziroglu (4) reported that, from the observation of their experiments, the flow downstream of the mixer was a well-mixed bubbly flow at steady-state operation. However, at the onset of instability, alternating bubbly slugs containing mostly air or mostly water was observed. This observation can be applied to the present blowdown tests to explain the pressure oscillations and the change in shape of the jet at the exit of the nozzle. In the unstable region, a higher pressure was measured when a slug of gas was passing through the locations of the pressure taps downstream of the nozzle and a lower pressure was measured when a slug of liquid was passing through the locations. Slugs of liquid were incompressible and slugs of gas were compressible, thus, alternating slugs containing mostly gas or mostly water would result in pressure oscillations and change in shape of the jet at the exit, (i.e., a circular column for an incompressible jet and a circular cone for a compressible jet). The density upstream of the orifice at the onset of instability was approximately 5.2 times the liquid density as reported by Stenning and Veziroglu. This would result in a void fraction upstream of the orifice of approximately 0.8. It is doubtful that the present system could attain such a high void fraction upstream of the nozzle. The pressure drop of the system used by Stenning and Veziroglu ($\sim 10^4$ Pa) was much smaller than that of the present system ($\sim 10^5$ Pa). It is possible that the larger pressure drop in the present system may cause the instability to occur at a relatively smaller void fraction than that observed by Stenning and Veziroglu. However, by increasing the pressure drop of the system, another phenomenon (i.e., critical flow) may occur before the transition of the flow regime described previously. We shall see that this phenomenon can be explained from critical flow viewpoint at much lower void fraction.

When critical flow is reached, the velocity at the throat of the nozzle equals the sonic velocity of a two-phase mixture. Figure 15 shows the variation of the

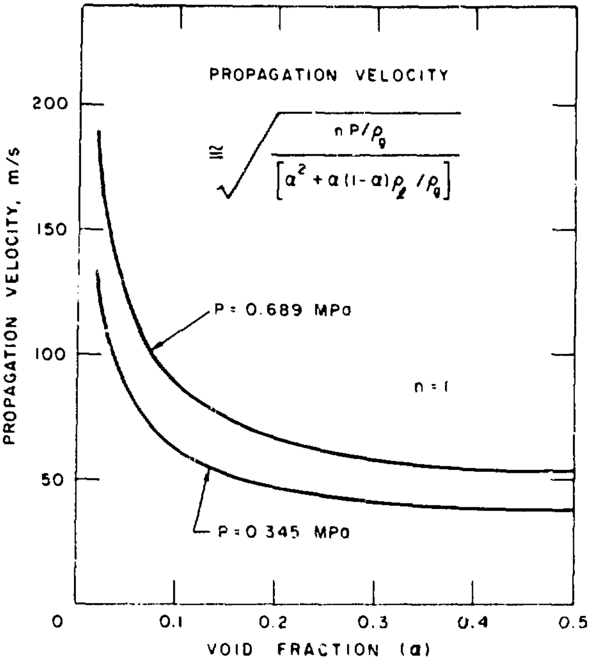

Fig.15 Variation of propagation velocity with void fraction in a two-phase mixture

sonic velocity with void fraction for a two-component two-phase mixture in the bubbly flow regime. Large variation in sonic velocity is observed for void fraction less than ~0.1. The critical pressure ratio η can be expressed in terms of the stagnation void fraction α_i, based on an equilibrium, homogeneous model for steady two-phase flow(6):

$$-\ln \eta = \left(\frac{1-\alpha_i}{\alpha_i}\right)\left(\frac{\eta^2}{2}\right) - \left(\frac{1-\alpha_i}{\alpha_i}\right)(1-2\eta) + 1/2 \qquad (23)$$

If $\alpha_i << 1$, equation (23) can be reduced approximately to the following equation:

$$\alpha_i = \frac{(1-2\eta) - [(2\eta-1)^2 - \eta^2(1+2\ln\eta)]^{1/2}}{1 + 2\ln\eta} \qquad (24)$$

The exit void fraction is

$$\alpha_e = \frac{1}{1 + (1-\alpha_i)\eta/\alpha_i} \qquad (25)$$

Calculated results by using equations (24) and (25) are shown in Fig. 16. If the inlet or stagnation void fraction is less than ~0.02, the exit void fraction will be less than ~0.1. Under these conditions a small disturbance in inlet void fraction will cause a relatively large change in discharge velocity as shown in Fig. 15. The change in discharge velocity will be fed back upstream to cause a change in inlet void and so on, thus, causing the flow to oscillate. The critical pressure ratio must be less than ~0.17 (which corresponds to α_i = 0.02) in order to have this kind of oscillation. The pressure ratios (i.e., the ratio of the peak of the large amplitude oscillation to the vessel pressure) observed in the present tests were approximately between 0.2 and 0.3, which were in the same order of magnitude as that required to cause oscillations.

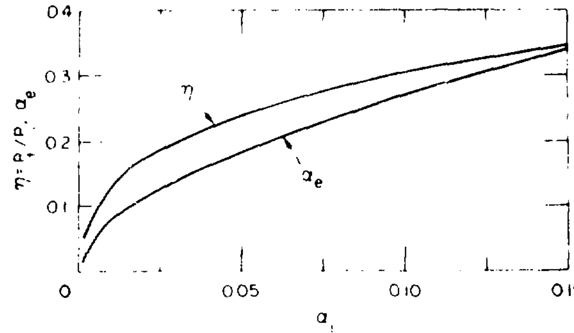

Fig.16 Variations of critical pressure ratio and exit void fraction with inlet (stagnation) void fraction in an equilibrium, homogeneous, steady, two-phase flow

SUMMARY AND CONCLUSIONS

(1) Experimental results with discharge nozzle A indicated that the dissolved gas did not significantly affect the discharge flow rate without providing additional surface area in the blowdown vessel. This observation was also true for discharge geometries B and C which had long pipe downstream of the nozzle, although nonperiodic, intermittent, pressure oscillations did occur. The time required to exhaust the water in the blowdown vessel was delayed slightly (up to ~10%) for tests with additional nitrogen dissolved in the system.

(2) Experimental results with tube bundle inside the blowdown vessel, which increased the surface area in contact with water by a factor of ~10, showed that the dissolved nitorgen caused large-amplitude pressure (and hence flow) oscillations downstream of the discharge nozzle for all three test sections and for the pressure range (1.48 MPa to 4.24 MPa) covered in the present tests. As a result of these oscillations, the time required to exhaust all the water in the blowdown vessel was increased by 20 to 30% over those tests where no additional nitrogen was being dissolved in water. The amplitude of oscillation increased with increaisng initial pressure in the blowdown vessel. The ratios of the peak pressure of oscillation to the pressure in the blowdown vessel at any instant were approximately 0.3 for tests with relative high initial pressure and it decreased slightly with decreasing initial pressure in the blowdown vessel. The frequency of oscillation was approximately 1 to 5 Hz.

(3) The simple analytical model described in this paper is able to predict the blowdown vessel pressure as accurately as one can assess the polytropic behavior of the initial gas volume in the vessel.

(4) The continuous large amplitude oscillations observed in some of the present tests were likely to be associated with the so-called density-wave oscillations which has the unique

characteristics that the frequency of oscillation is inversely proportional to the residence time. These oscillations can be explained from critical flow viewpoint.

ACKNOWLEDGEMENTS

The authors wish to thank Dr. Y. Y. Hsu of the Nuclear Regulatory Commission for initiating this work. The assistance received from Messrs. R. L. S. aniel, D. J. Quinn, and E. A. Spleha during construction of the experimental apparatus and testing are also acknowledged.

REFERENCES

1 Westwater, J. W., "Measurements of Bubble Growth During Mass Transfer," in Cavitation in Real Liquids, Davis, R., ed., Elsevier, New York, 1964, pp. 34-54.

2 Cha, Y. S. and Henry, R. E., "Effects of Dissolved Gas During Blowdown of a Subcooled Liquid," ANL Report, to be published.

3 Streeter, V. L. and Wylie, E. B., Hydraulic Transients, McGraw-Hill, 1967, pp. 13-14.

4 Stenning, A. H. and Veziroglu, T. N., "Oscillations in Two-Component Two-Phase Flow," NASA-CR-72121, 1967.

5 Stenning, A. H. and Veziroglu, T. N., "Flow Oscillation Modes in Forced-Convection Boiling," Proceedings of the 1965 Heat Transfer and Fluid Mechanics Institute, Stanford University Press, 1965, pp. 301-316.

6 Henry, R. E., "Gas Detection With A Choked Converging-Diverging Nozzle," Transaction of American Nuclear Society, Vol. 13, 1970, pp. 794-795.